Electronic Supplementary Information

$NiMn_2O_4$ spinel binary nanostructure decorated on three-dimensional reduced graphene oxide hydrogel for bifunctional materials in non–enzymatic glucose sensor

Yen-Linh Thi Ngo[1], Lijun Sui[1,2], Wei Ahn[1,2], Jin Suk Chung[1] and Seung Hyun Hur[1,*]

[1]School of Chemical Engineering, University of Ulsan, Daehak-ro 93, Nam-gu, Ulsan 44610, Republic of Korea.

Fax: +82-52-259-1028; Tel: +82-52-259-1689

*E-mail: shhur@ulsan.ac.kr

[2]College of Chemistry and Chemical Engineering, Shanghai University of Engineering Science, Shanghai 201620, PR China

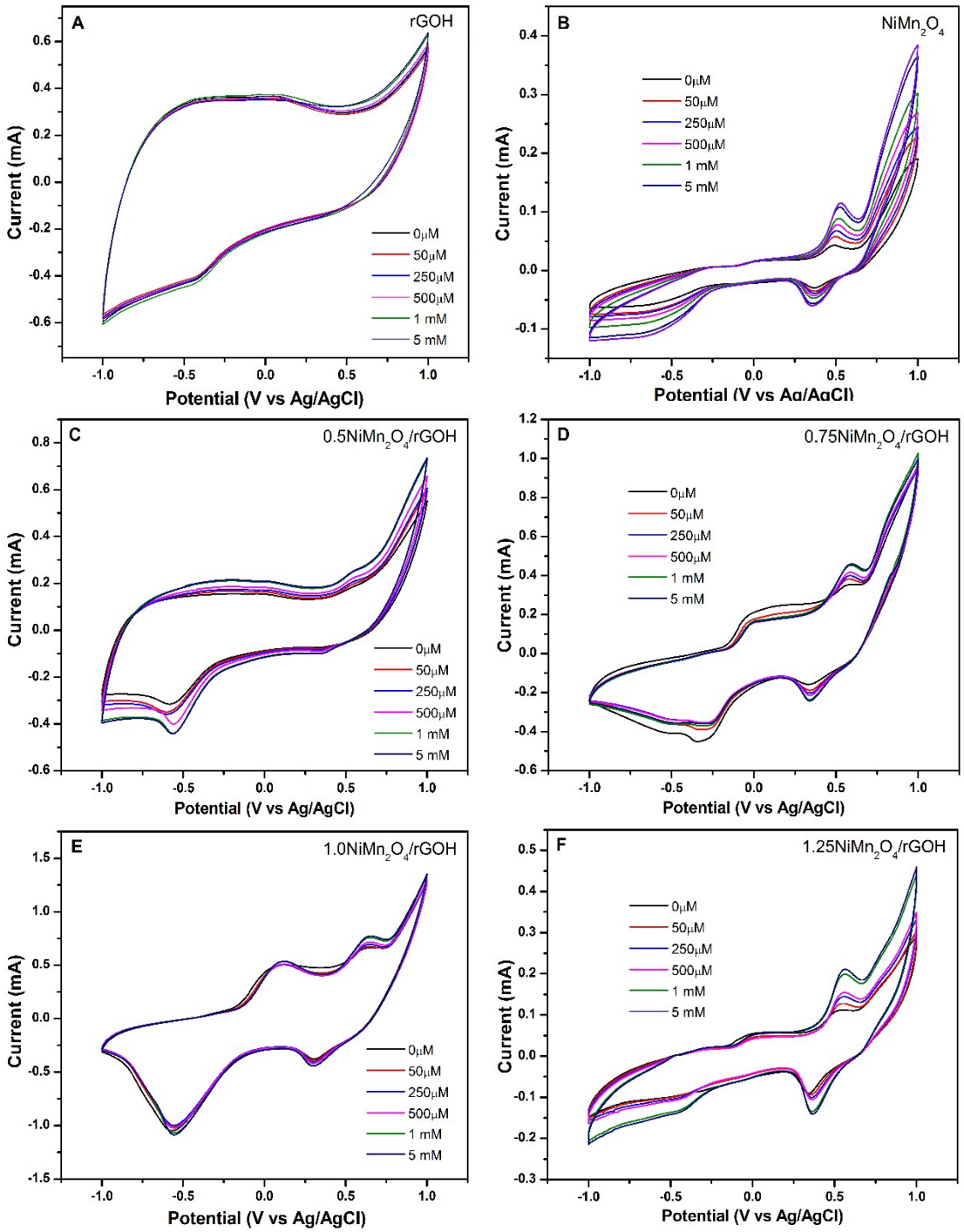

Fig. S1. (A-F) CV curves of rGOH (A), $NiMn_2O_4$ (B), and the $NiMn_2O_4$/rGOHs (C-F) modified electrodes synthesized at different $NiMn_2O_4$ contents at various glucose concentrations in a 0.1 M NaOH at a scan rate of 50 mV/s.

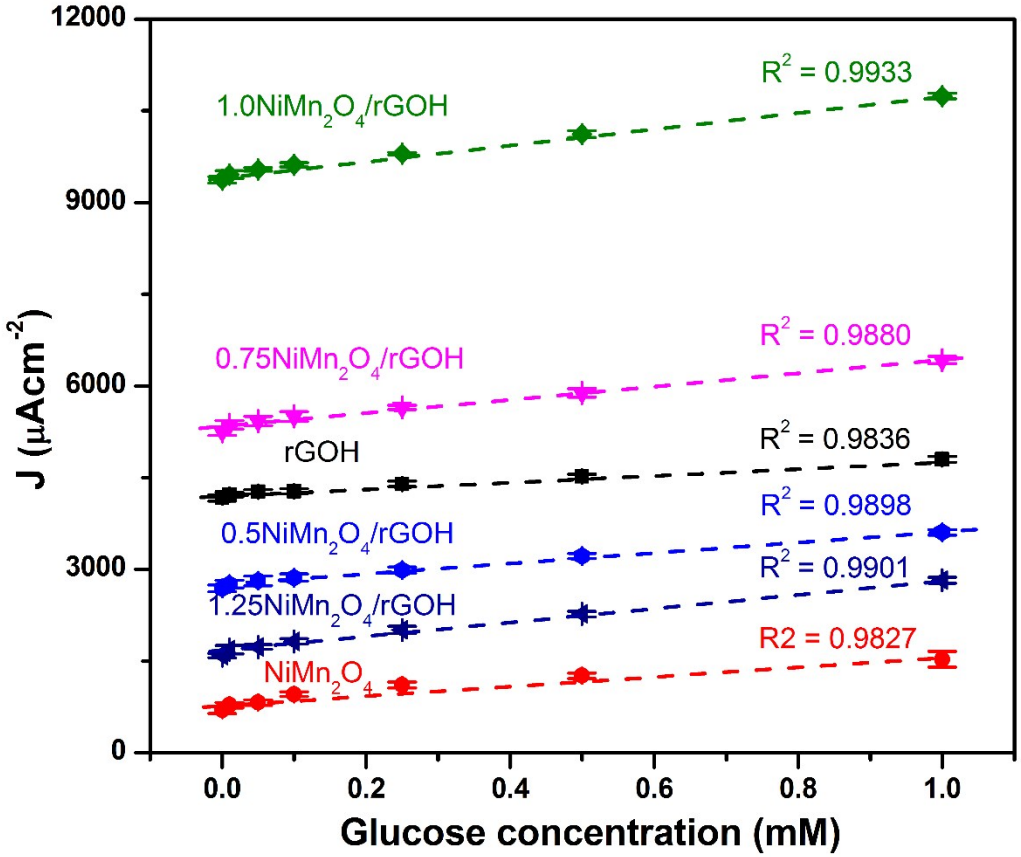

Fig. S2. Calibration curves of sensitivity vs. concentration of glucose of the $NiMn_2O_4$/rGOH synthesized at different $NiMn_2O_4$ contents in a 0.1 M NaOH at a scan rate of 50 mV/s.

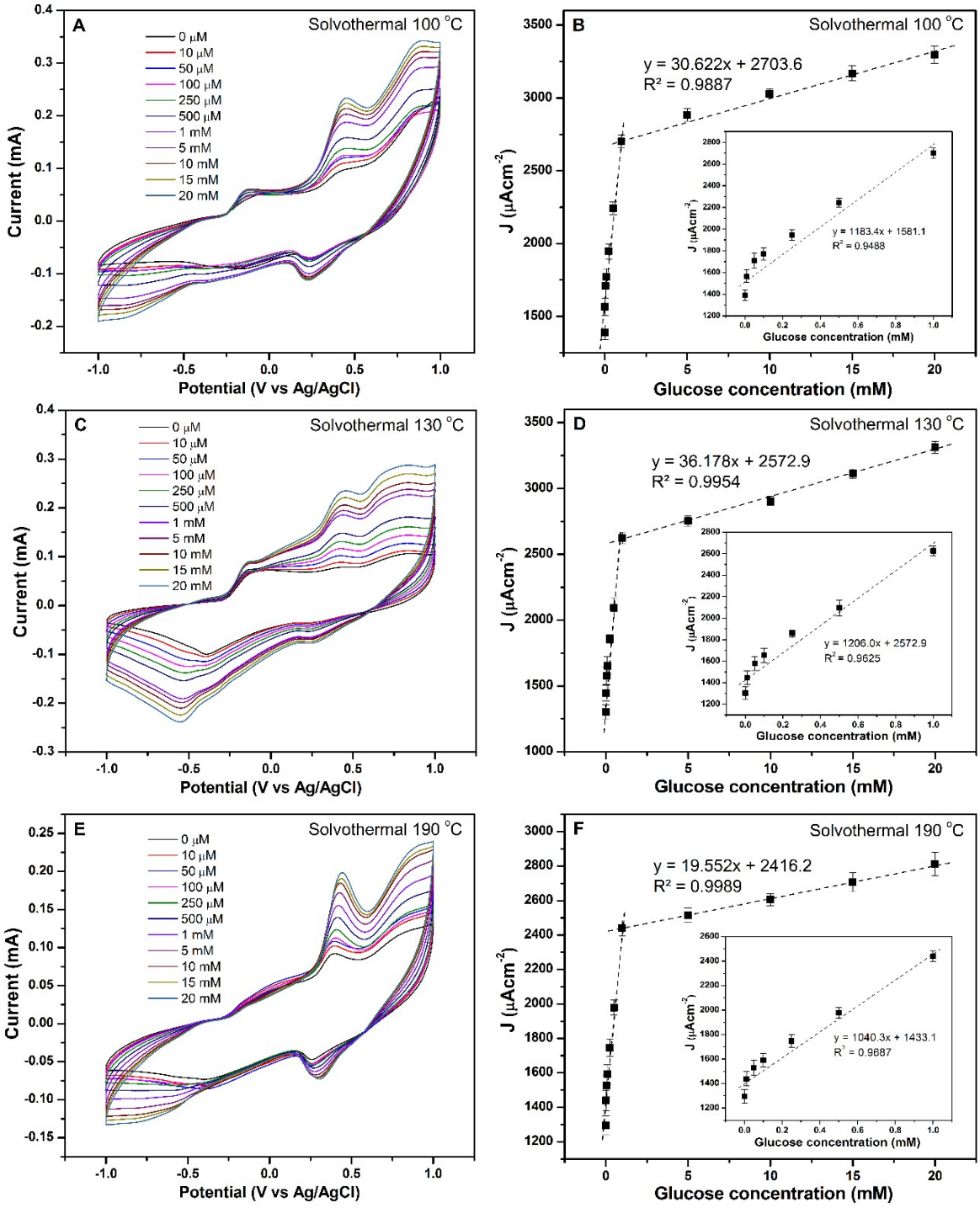

Fig. S3. (A-C-E) CV curves and (B-D-F) corresponding calibration curves of sensitivity vs. concentration of glucose of the 1.0$NiMn_2O_4$/rGOH electrodes synthesized at different solvothermal temperature in a 0.1 M NaOH at a scan rate of 50 mV/s.

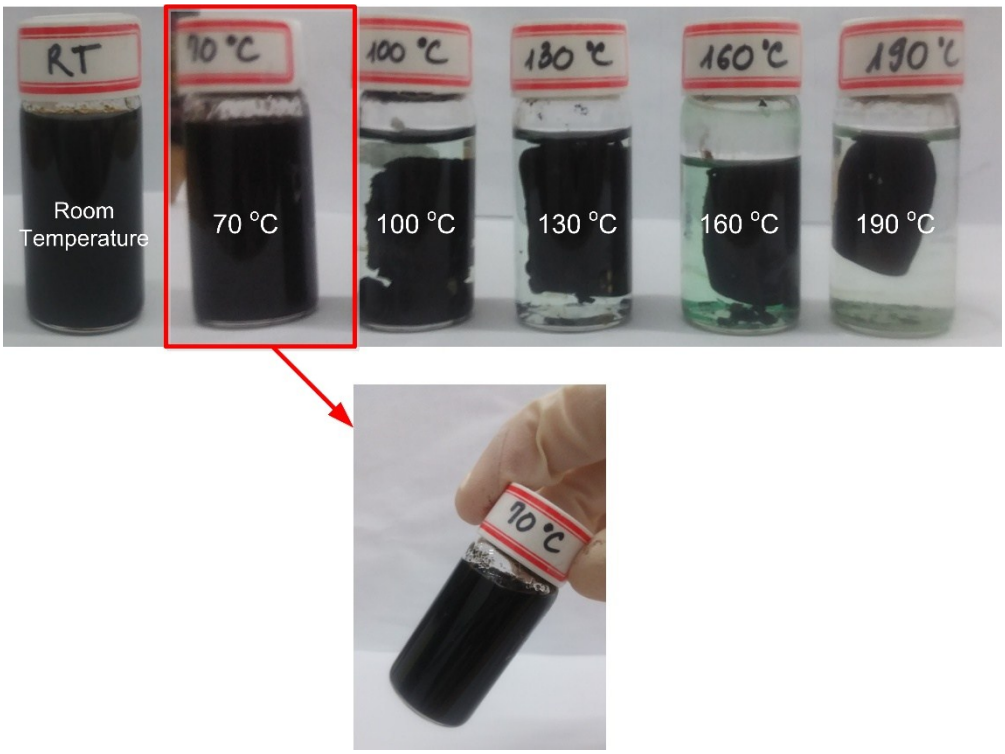

Fig. S4. The images of various $NiMn_2O_4$/rGOH prepared at different solvothermal temperature. Only above 130 °C the hydrogel can be properly formed and at too high temperature hydrogel becomes hard and thus the specific area decreases (Table S2). Therefore, we fabricated all samples for further study in this manuscript at 160 °C.

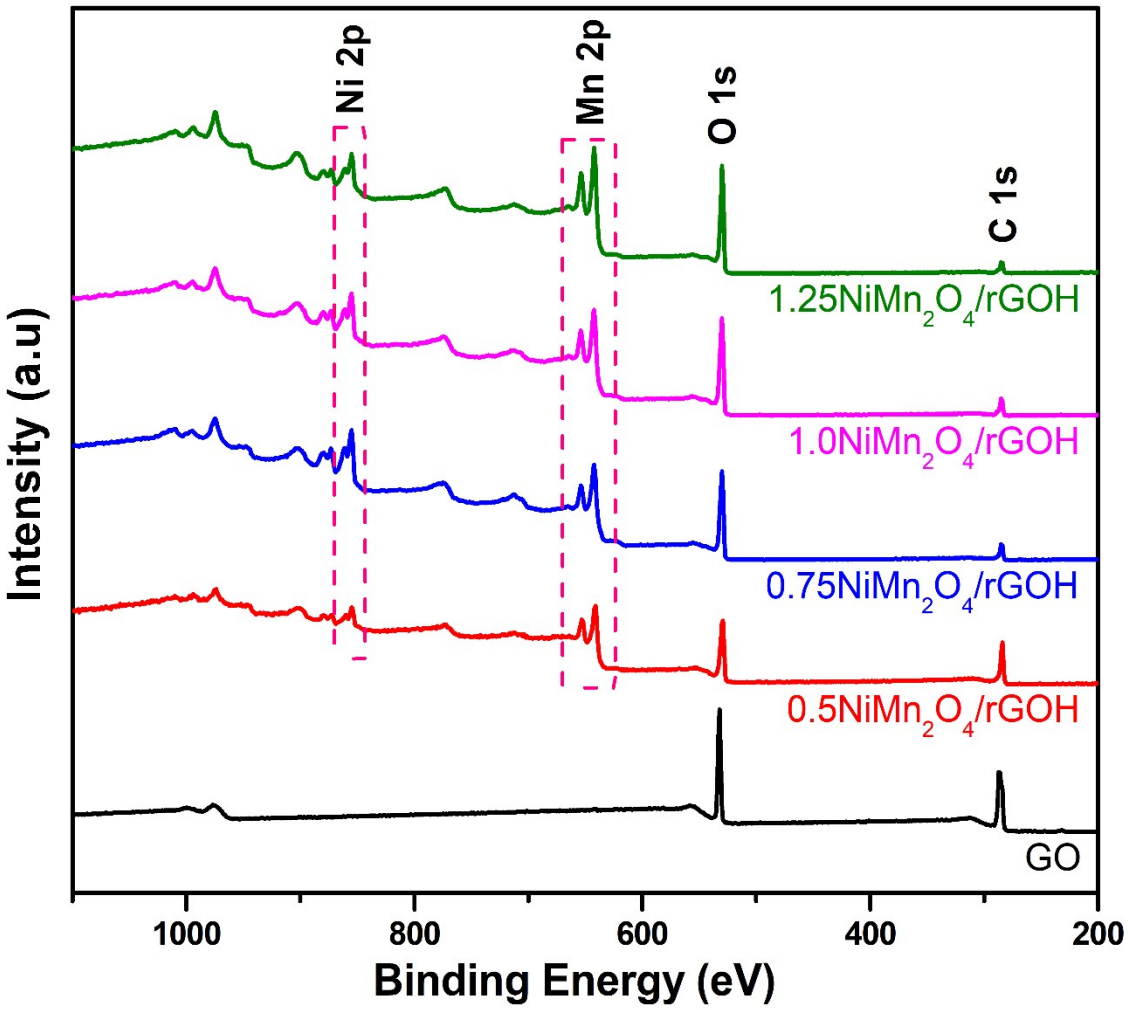

Fig. S5. The XPS survey spectra of various $xNiMn_2O_4$/rGOH fabricated at 160 °C.

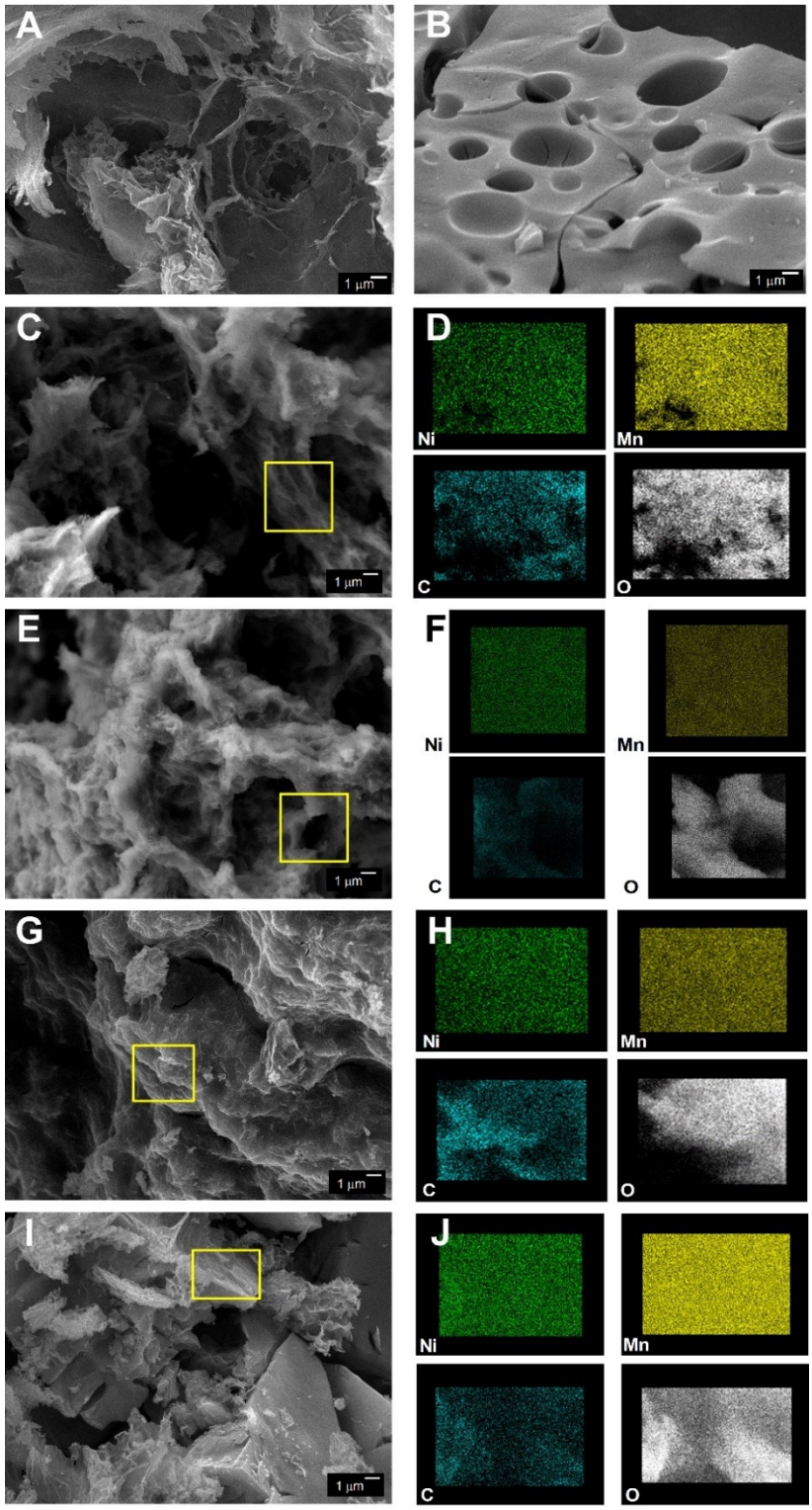

Fig. S6. FE-SEM images of (A) rGOH, (B) $NiMn_2O_4$, and FE-SEM/EDAX images for Ni, Mn, C and O elements of (C-D) $0.5NiMn_2O_4$/rGOH, (E-F) $0.75NiMn_2O_4$/rGOH, (G-H) $1.0NiMn_2O_4$/rGOH and (I-J) $1.25NiMn_2O_4$/rGOH.

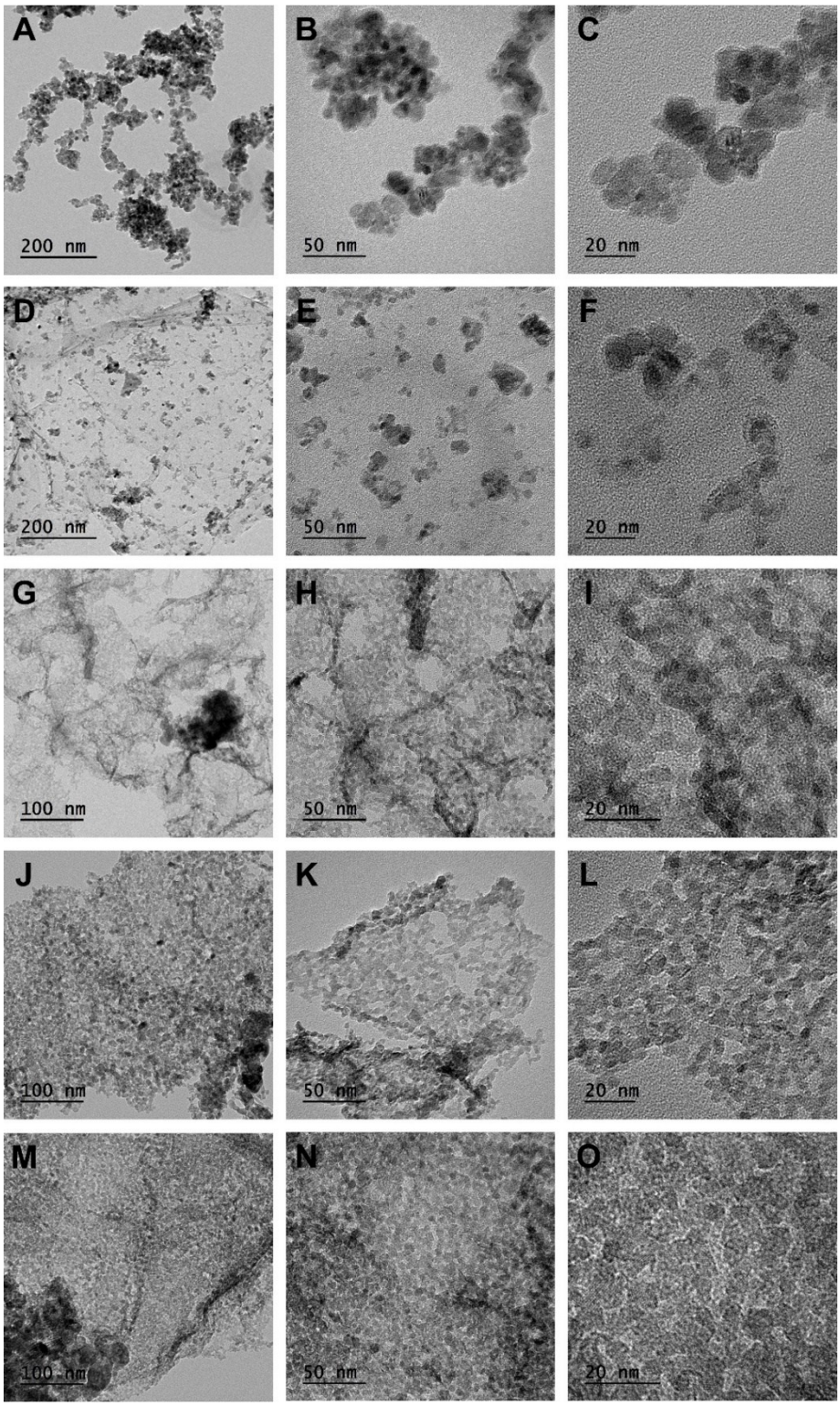

Fig. S7. HR-TEM images of (A-C) $NiMn_2O_4$, (D-F) $0.5NiMn_2O_4$/rGOH, (G-I) $0.75NiMn_2O_4$/rGOH, (J-L) $1.0NiMn_2O_4$/rGOH and (M-O) $1.25NiMn_2O_4$/rGOH at various resolution.

Table S1. BET surface areas of rGOH, $NiMn_2O_4$ and various $NiMn_2O_4$/rGOHs of different $NiMn_2O_4$ contents

Sample	Content of $NiMn_2O_4$ (mmol)	BET surface area (m^2/g)
rGOH	0	404.35
$NiMn_2O_4$	1.00	100.10
0.5$NiMn_2O_4$/rGOH	0.50	243.13
0.75$NiMn_2O_4$/rGOH	0.75	277.81
1.0$NiMn_2O_4$/rGOH	1.00	347.14
1.25$NiMn_2O_4$/rGOH	1.25	308.17

Table S2. BET surface areas of various 1.0$NiMn_2O_4$/rGOHs synthesized at different solvothermal temperatures.

Sample	Temperature (°C)	BET surface area (m^2/g)
1.0$NiMn_2O_4$/rGOH	100	215.16
	130	263.19
	160	347.14
	190	183.20

Table S3. The glucose sensing results of our study compared to those of the previous nickel/ manganese oxide based studies.

Material electrode	Linear range	Sensitivity ($\mu A.mM^{-1}cm^{-2}$)	Low detection limit (LOD)	Response time (s)	Ref.
Hedgehog-NiO	0.1 – 5 μM	1052.8	1.2 μM	–	[38]
NiO/rGO	3.13 μM – 3.05 mM	1087	1 μM	~ 10	[39]
NiO-Nanofibers/rGO	0.002 – 0.6 mM	1100	0.77 μM	< 5	[40]
NiO/MWCNT	0.2 – 12 mM	–	160 μM	10	[41]
Ni/MnO_2	0.25 μM – 3.5 mM	1040	0.1 μM	~3	[42]
MnO_2/MWCNT	10 μM – 28 mM	33.19	–	10	[4]
MnO_2/Graphene	0.04 – 2 mM	3300	10 μM	10	[5]
$NiMn_2O_4$/rGOH	Up to 1 mM 1 mM – 20 mM	1310.8 59.24	1.78 μM 0.82 mM	< 3.5	This work

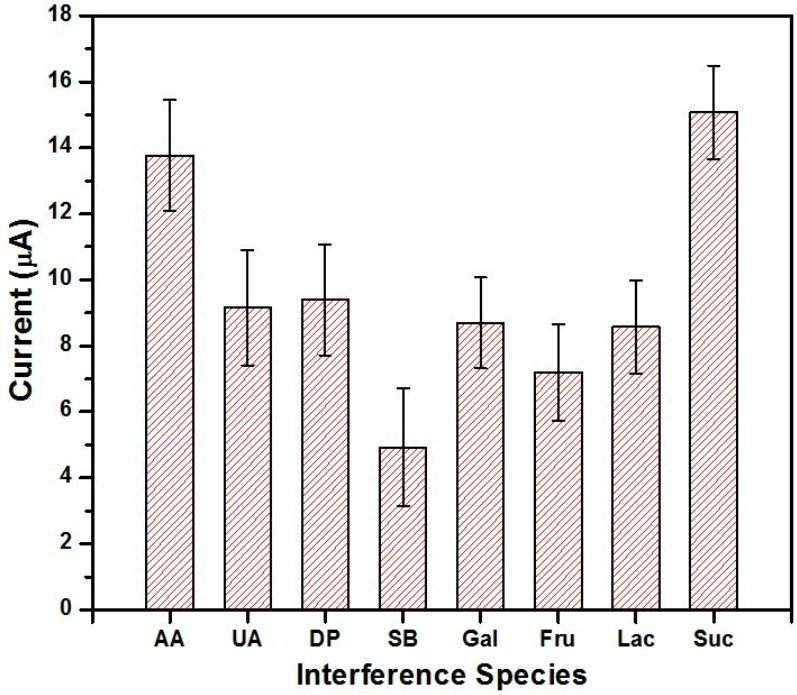

Fig. S8. The current increase of 1.0$NiMn_2O_4$/rGOH electrode when 5 mM of each interfering species was injected in 0.1 M NaOH electrolyte at the applied voltage of + 0.62 V. The error bars indicate the standard deviation of triplicate determination of each interfering species.

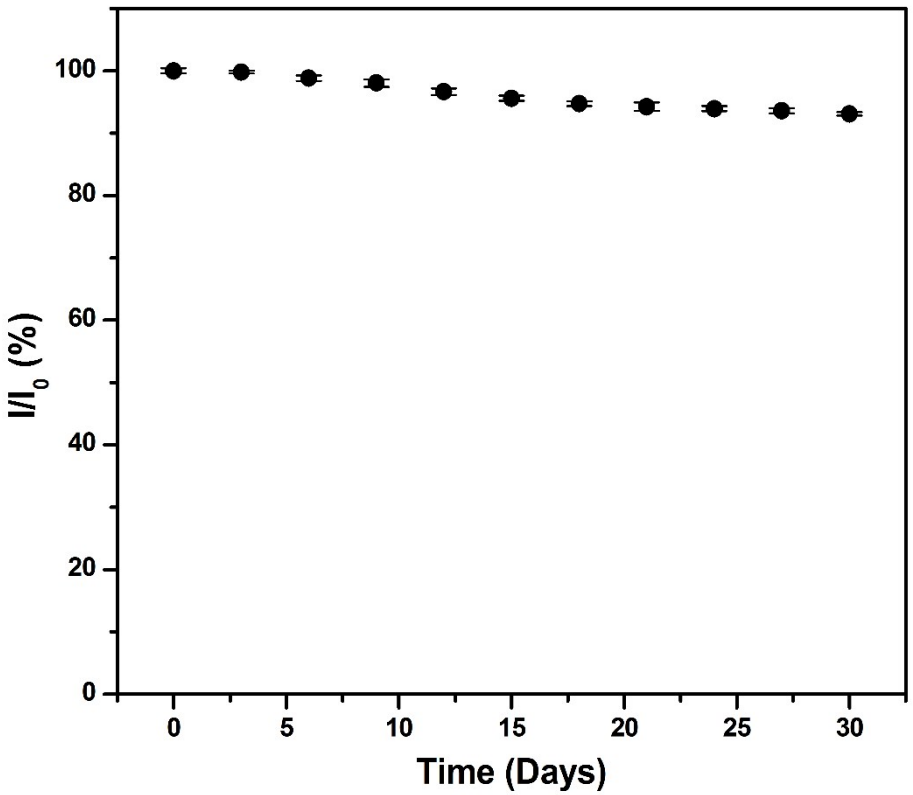

Fig. S9. Stability of the 1.0$NiMn_2O_4$/rGOH based on glucose sensor at room temperature. The current was measured every 3 days for one month.

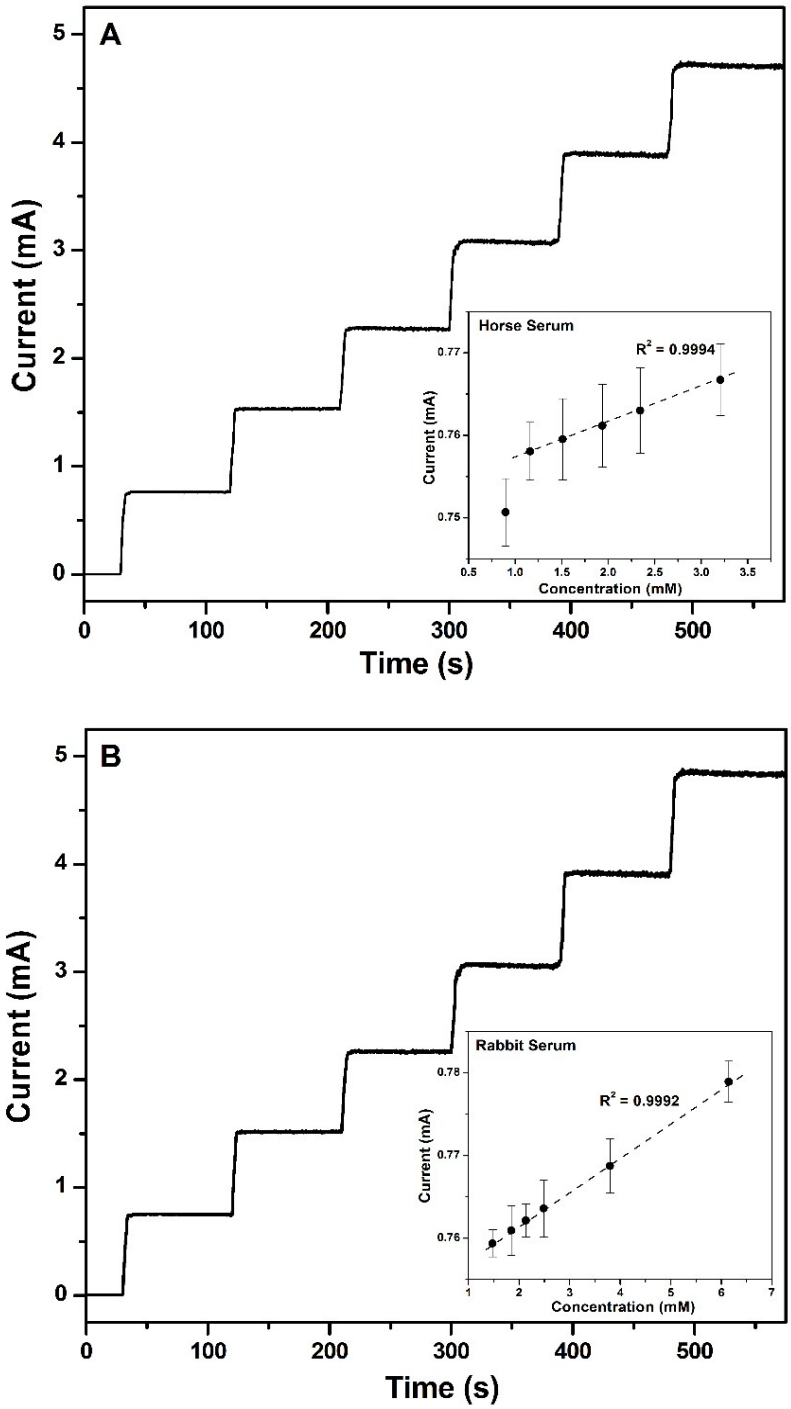

Fig. S10. Amperometric tests of $1.0NiMn_2O_4$/rGOH in 0.1 M NaOH at + 0.62 V with the successive addition of (A) Horse and (B) Rabbit serum.

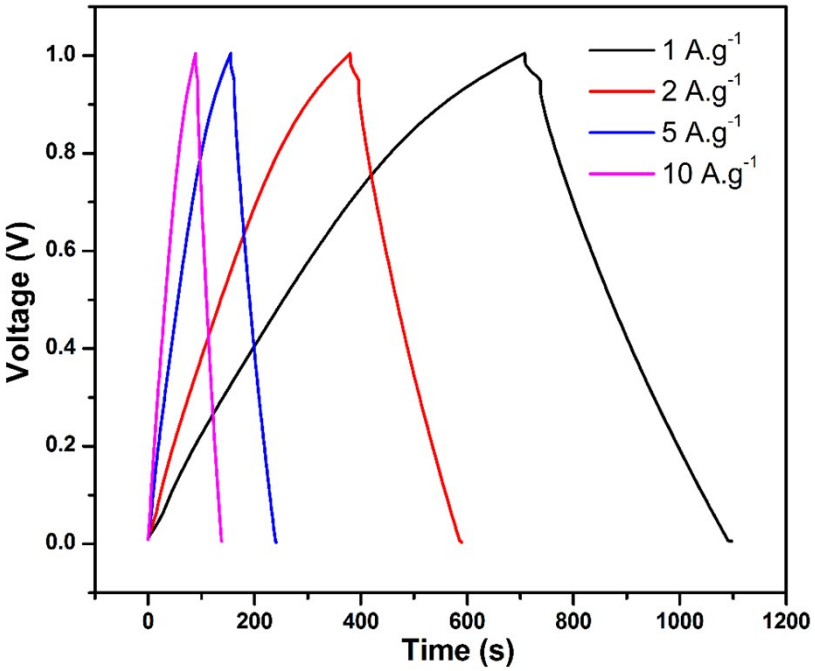

Fig. S11. Galvanostatic charge-discharge (CD) curves of 1.0$NiMn_2O_4$/rGOH at 1, 2, 5 and 10 $A \cdot g^{-1}$.

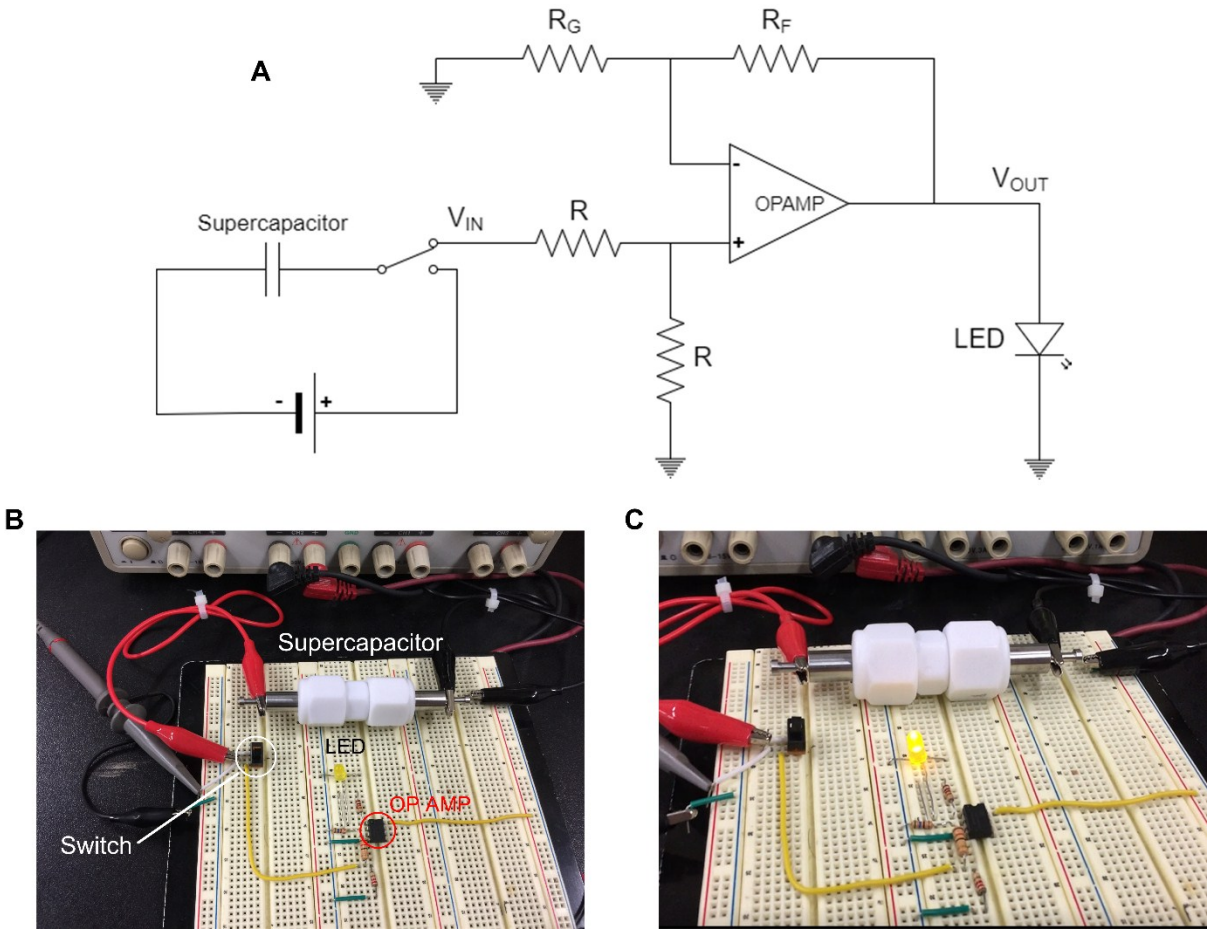

Fig. S12. (A) The electric diagram of $NiMn_2O_4$/rGOH as power supply to turn on LED lamp. (B) before and (C) after supplying power to LED by $NiMn_2O_4$/rGOH supercapacitor fabricated in this study.

The operation procedure of self-powered glucose sensor

In this experiment, the $NiMn_2O_4$/rGOH was used as both sensing and supercapacitor (SC) electrodes. Firstly, a DC power supply was turned on and charged the SC fabricated in this study at 2.5V for 45s. Then, the DC power was turned off and only charged SC supplied the power to electrochemical cell for glucose detection. The current was measured before and after adding 0.1 mM of glucose with amperemeter.

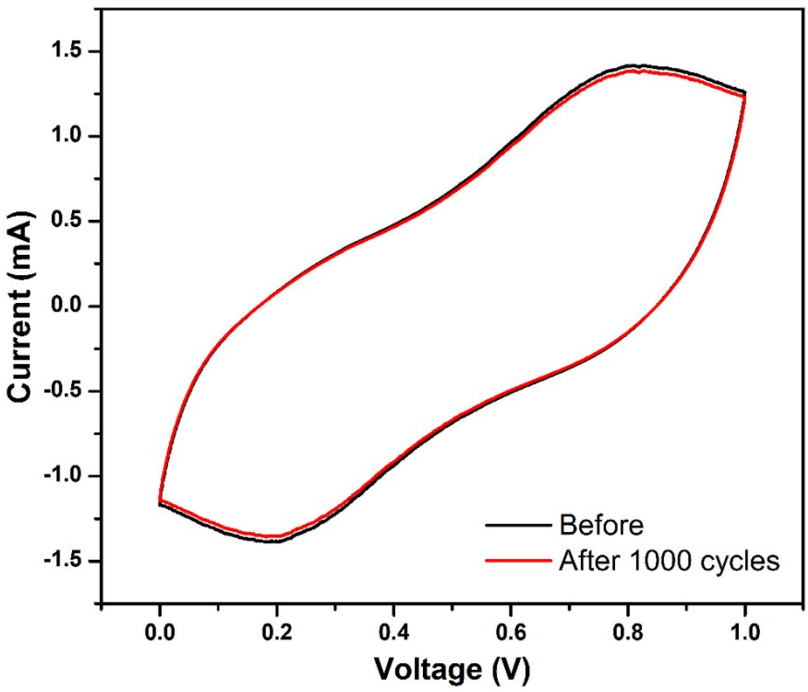

Fig. S13. The CV curves before and after 1000 cycles of 1.0$NiMn_2O_4$/rGOH electrode.